

PFC/JA-86-59

**Extraordinary Mode Absorption at the
Electron Cyclotron Harmonic Frequencies as a
Tokamak Electron Temperature Diagnostic**

A. Pachtman, S. M. Wolfe, I. H. Hutchinson

Plasma Fusion Center
Massachusetts Institute of Technology
Cambridge, MA 02139

November 1986

Submitted to: Nuclear Fusion

This work was supported by the U. S. Department of Energy Contract No. DE-AC02-78ET51013. Reproduction, translation, publication, use and disposal, in whole or in part by or for the United States government is permitted.

By acceptance of this article, the publisher and/or recipient acknowledges the U. S. Government's right to retain a non-exclusive, royalty-free license in and to any copyright covering this paper.

EXTRAORDINARY MODE ABSORPTION AT THE ELECTRON CYCLOTRON HARMONIC FREQUENCIES AS A TOKAMAK ELECTRON TEMPERATURE DIAGNOSTIC

A. PACHTMAN,* S.M. WOLFE, I.H. HUTCHINSON (Plasma Fusion Center, Massachusetts Institute of Technology, Cambridge, Massachusetts, United States of America)

ABSTRACT. An experimental study of Extraordinary mode plasma absorption at the semi-opaque second and third electron cyclotron harmonic frequencies has been performed on the ALCATOR C Tokamak. A narrow beam of submillimeter laser radiation was used to illuminate the plasma in a horizontal plane, providing a continuous measurement of the one-pass, quasi-perpendicular transmission. Experimental electron cyclotron absorption (ECA) data has been found to agree with lowest significant order finite density and finite Larmor radius theoretical results. ECA data has been used along with Tokamak electron density and magnetic field data to determine local electron temperatures in the range $75 \leq T_e(\text{eV}) \leq 3300$, with a spatial resolution ≤ 1 cm. Transmission during Lower Hybrid frequency RF Heating and Current Drive remained unaffected by suprathermal electrons due to their low density and the relativistic downshift of the absorption line. This allowed the ECA technique to be used to measure the bulk plasma temperature during Lower Hybrid RF Heating. A density dependent non-resonant attenuation was observed which, when present, was taken into account in the data analysis.

1. Introduction

The practical importance of radiation phenomena in the electron cyclotron resonance (ECR) range of frequencies was recognized early on in controlled thermonuclear fusion research and throughout its development. Although cyclotron absorption studies relating to ECR Heating abound in the literature, there have been

* Present Address: Shanghai Institute of Optics and Fine Mechanics, Shanghai, People's Republic of China.

relatively few studies of expressly plasma diagnostic intent, and these have been limited in depth and scope. In this paper, the unique plasma diagnostic capabilities offered by electron cyclotron harmonic absorption in a hot, dense, Tokamak plasma are demonstrated. The ranges of density, temperature, and frequency investigated approach those expected for future high field ignition devices, under a variety of reactor relevant conditions, such as during RF Heating and Current Drive.

For the conditions of this work, lowest WKB and finite Larmor radius (FLR) order formulations [1,2] were found to be sufficient to describe absorption by a Maxwellian plasma for semi-opaque second and third harmonics. For a semi-opaque harmonic $n \geq 2$, the Extraordinary (X) mode optical depth

$$\tau_{n,X} = -\ln(T_{n,X}) \leq 1,$$

where $T_{n,X}$ is the transmission, is directly related to the electron density n_e , electron temperature T_e , and magnetic field B_t at the resonance location, via the factor $n_e T_e^{n-1} / B_t^n$. This proportionality forms the basis for diagnosing the local plasma temperature by measuring the plasma transmission, given data on the Tokamak density and magnetic field, which are in general readily obtainable. The Tokamak toroidal magnetic field varies in space as

$$B_t(r) = B_t(0) \frac{R}{R + r \cos \theta},$$

where, in ALCATOR C, $R = 64$ cm is the major radius, $r = 16.5$ cm is the minor radius, and $\cos \theta = 1$ in the toroidal midplane. Due to the narrow relativistic absorption linewidth for quasi-perpendicular propagation [1] and the spatial variation of the magnetic field, an unambiguous position-frequency correspondence exists in the plasma for the conditions of the present experiment, with a spatial resolution of 1 cm or less for the absorption.

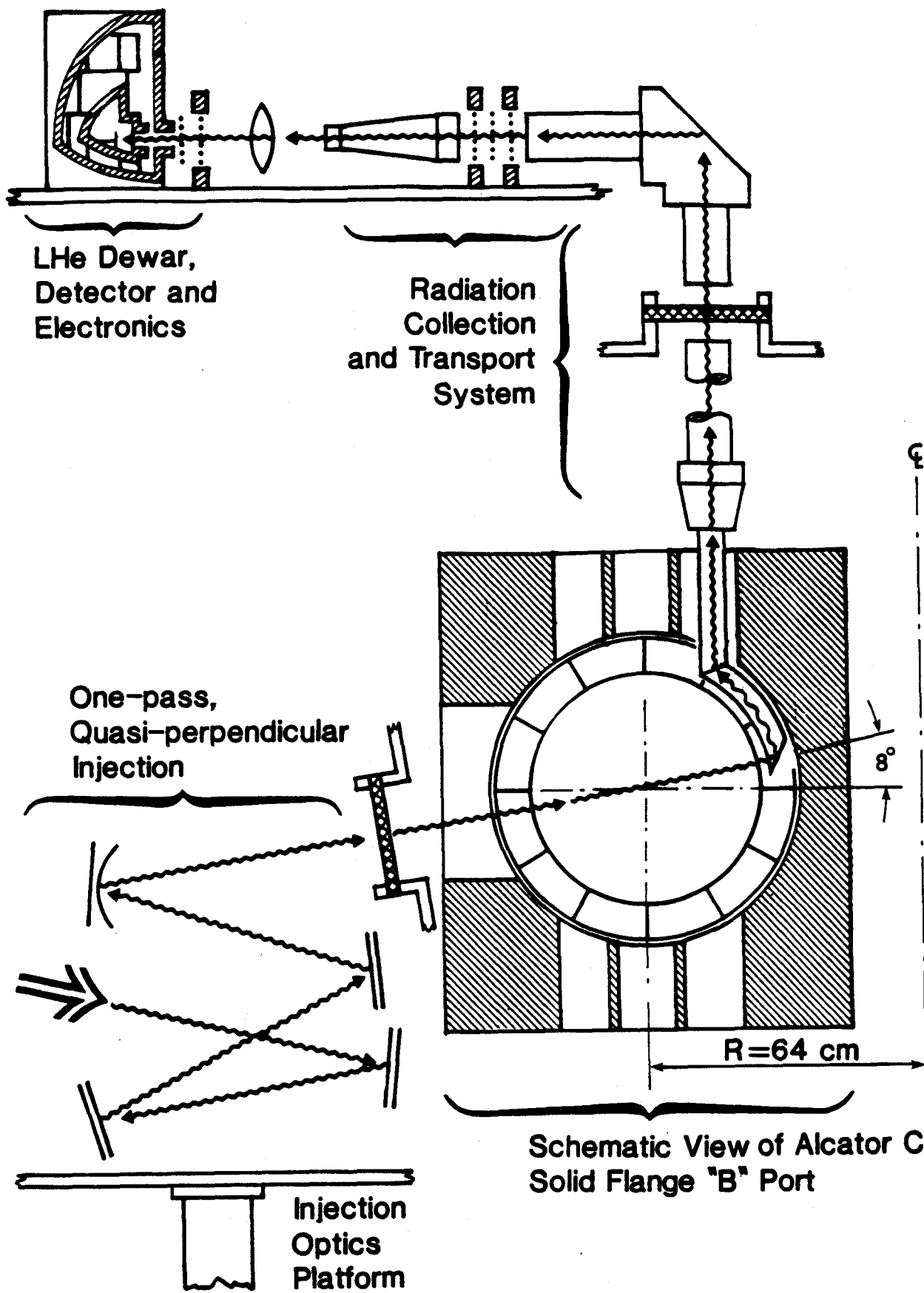
Furthermore, due to the low densities of suprathreshold electron components found in ALCATOR C, and the strong relativistic downshift of the absorption line away from the central harmonic resonance frequency for these electrons, the transmission remained unaffected by these components. This circumstance allowed the transmission to be used as a bulk plasma temperature diagnostic during RF injection.

2. Experiment Configuration

Radiation near 700 GHz in the electron cyclotron harmonic frequency range was produced by an optically pumped waveguide laser system located in the AL-CATOR C cell on an enclosed laser table, adjacent to the Tokamak. Molecular laser lines in Formic acid, HCOOH, and its deuterated analog, DCOOD, were used. A novel FIR laser design was implemented which used a suspended counterweight to balance the atmospheric force acting on the laser vacuum window, which also served as the output coupler, so that laser cavity adjustments could be accomplished.

The experiment configuration and components are shown schematically in fig. 1. The probe radiation was transported from the laser to the Tokamak in free space as a Gaussian beam, and was brought to a focus at the back wall of the plasma chamber. There the radiation was coupled into a 1.4 cm diameter silver plated steel waveguide assembly, which conducted the radiation out of the Tokamak. From the device, the radiation was led in circular copper waveguide to an InSb photoconductive detector. The collected radiation, which included the plasma emission, was filtered by a triple metal mesh Fabry-Perot filter and a commercial low pass filter prior to detection. The filters passed a band of approximately 50 GHz about the laser frequency, which allowed third harmonic emission to be received from the central 5 cm region of the plasma. Data produced by the experiment was digitized at 5 kHz, and archived by a VAX 11/780 computer. The high working frequency and restricted diagnostic access conditions of the experiment represent a novel application of overmoded circular metallic waveguide propagation. The high transmissions measured for the various waveguide assemblies, with $.4 \leq \alpha(\text{dB/m}) \leq 1.3$, result from the relatively low losses of the characteristic modes of the circular metallic waveguide.

The FIR probe beam was chopped at 100 Hz to distinguish it from the more slowly varying plasma emission background also present in the signal. A portion of the beam was diverted at the laser to a power monitor, which provided a power reference signal. With these data, changes in the laser power were divided out of the raw transmission, and the absolute plasma transmission was thereby obtained.



1. Experiment configuration and components. Shown are the injection geometry, Tokamak cross section, waveguide assemblies, and filtering and detection assemblies.

Data was reduced by a "boxcar analyzer" routine which performed a synchronous integration of the modulated raw transmission and reference data, and generated plots of absolute transmission versus time.

Once the absolute plasma transmission at a given laser frequency was obtained, the electron temperature at the location of the n^{th} harmonic resonance was extracted using the fundamental $n_e T_e^{m-1} / B_t'$ scaling of the X mode optical depth. From the laser frequency and the toroidal field, the resonant position was calculated, and the local density was obtained from multichord interferometer data. The local temperature was then calculated from the measured optical depth. Furthermore, with harmonic emission data which was simultaneously collected in the experiment, information about the radiation temperature was deduced.

Each of the three experimentally measured parameters n_e , B_t , and $T_{n,X}$ which enter the electron temperature analysis introduces an uncertainty in the temperature which results. The overall temperature uncertainties in the regime of this work are in the 10% to 21% range for measurements in the interior plasma region $r < 12$ cm, and in the 50% to 100% range for the edge temperature measurements, due to the higher uncertainty in the density near the plasma edge. The range of applicability of the experimental method is limited at low density and temperature by a deteriorating accuracy due to low absorption. For absorptions of 10% or below, a 5% uncertainty in the third harmonic transmission causes an uncertainty in the temperature of 30% or greater [6]. Another limit is encountered at high density, due to interference from Marfes [3]. A Marfe is a cold, high density plasma region which forms near the plasma edge when the ratio of central electron density to plasma current exceeds a threshold value. Marfes scatter submillimeter radiation very efficiently due to the large density gradients present in the Marfe region. In addition, a steady non-resonant attenuation was observed under certain conditions which must be divided out of the transmission prior to obtaining the temperature. When required, this additional analysis increased the third harmonic temperature uncertainty by a factor of 1.4.

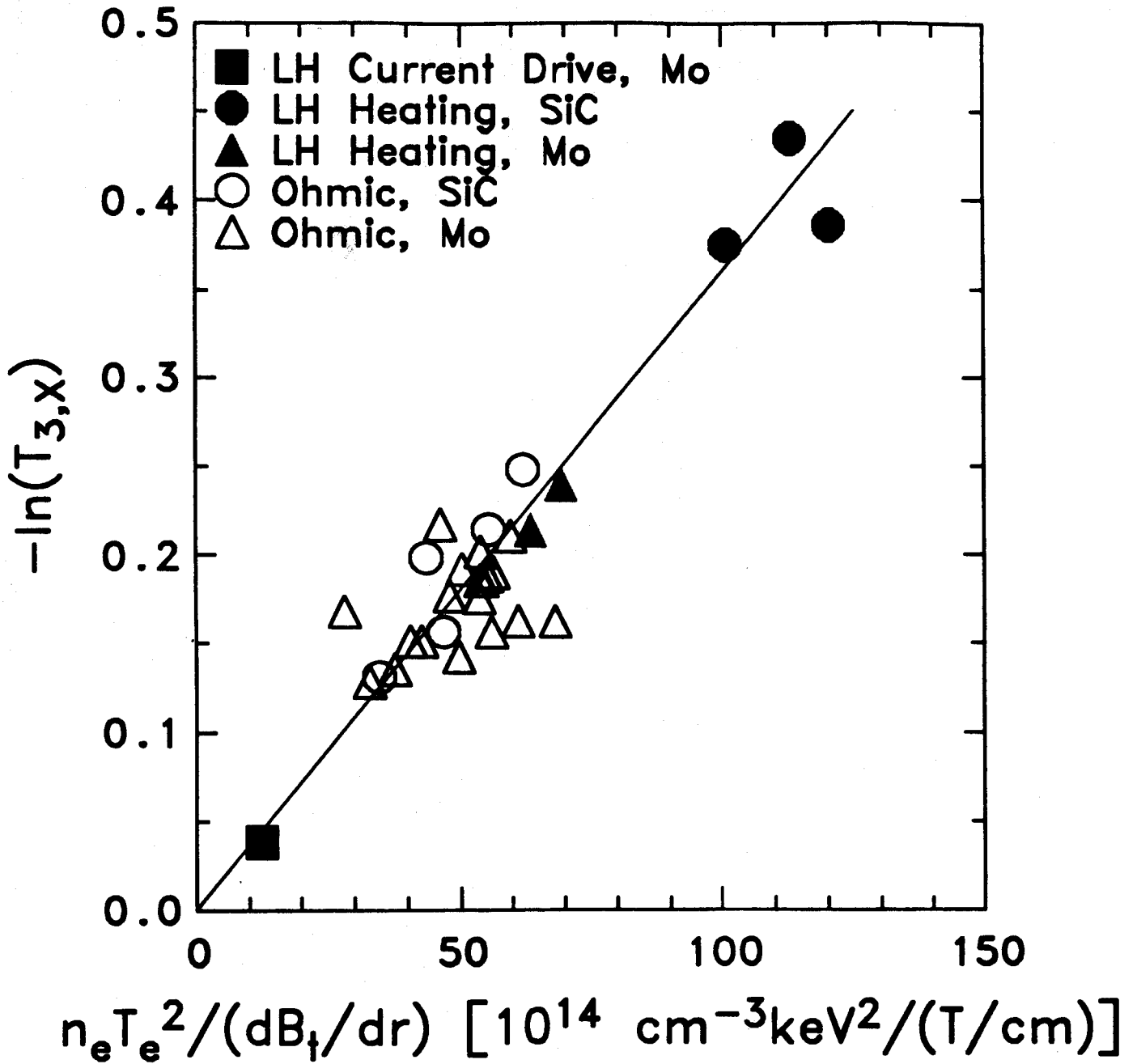
3. Results

Cyclotron harmonic transmission measurements have been carried out for a wide range of plasma conditions. Experimental transmission data with the third harmonic located at the plasma center agrees with lowest significant order finite density and FLR theoretical results, and follows the $n_e T_e^2 / B_t'$ scaling from 1.2 to 12×10^{15} [$\text{cm}^{-3} \text{keV}^2 / (\text{Tesla}/\text{cm})$], as shown in fig. 2. Data in the range $1.5 \leq T_e$ (keV) ≤ 3.3 , $.6 \leq \bar{n}_e (10^{14} \text{cm}^{-3}) \leq 3.1$, and $B_t = 8$ and 9 Tesla have been included, with temperatures obtained from Thomson scattering or second harmonic X mode electron cyclotron emission (ECE). Experiment conditions are designated in the legend as Ohmic Heating, or Lower Hybrid RF Heating or Current Drive, with either molybdenum or silicon carbide limiters. Each point represents one set of plasma conditions.

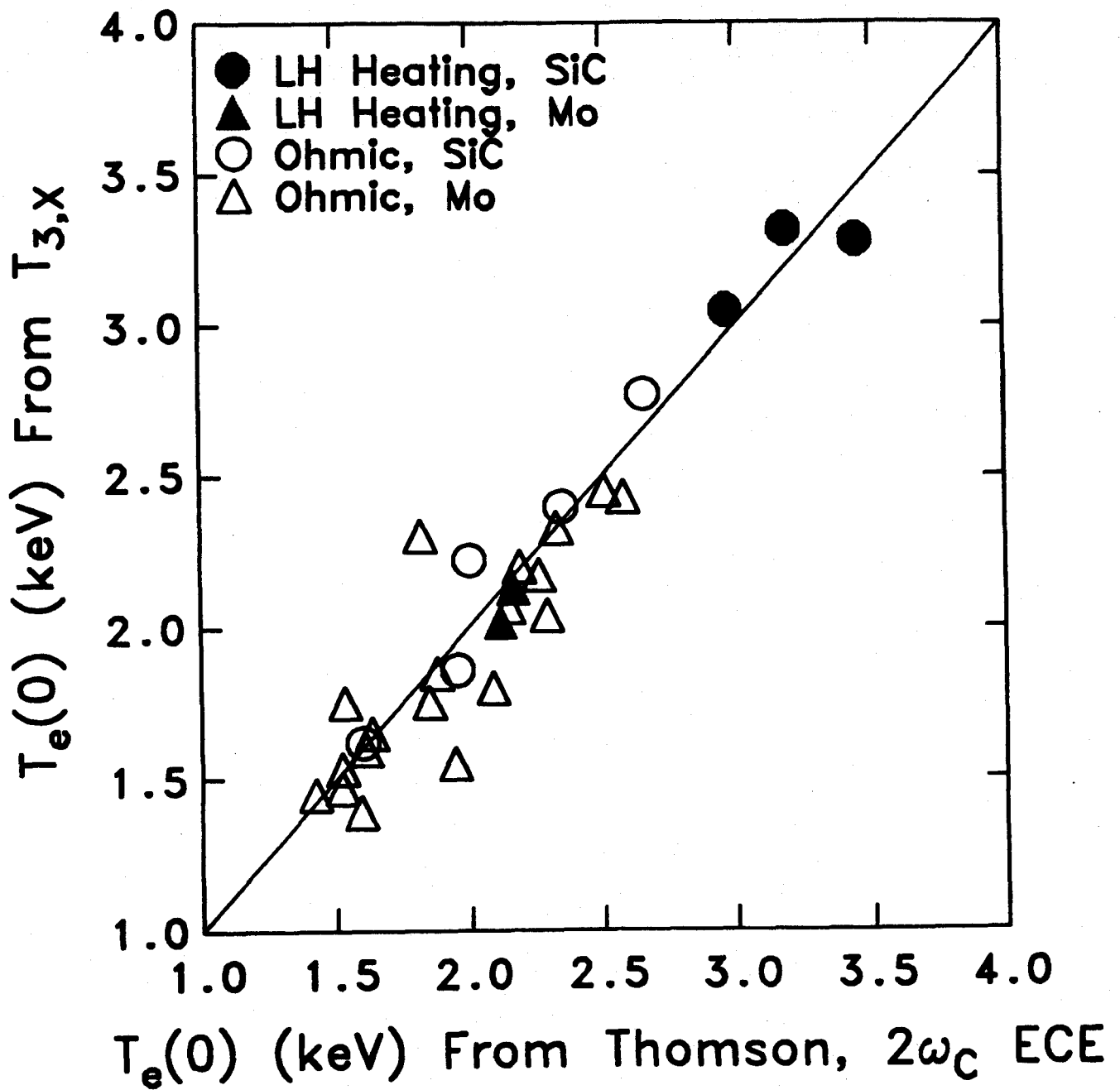
The above data may be presented in a manner which allows an evaluation of the ECA transmission technique as a diagnostic of electron temperature. In fig. 3, the central temperature obtained from third harmonic transmission data is directly plotted versus the temperatures reported by Ruby laser Thomson scattering or second harmonic ECE diagnostics on the same shots. Agreement is seen over the range of temperatures and plasma conditions shown.

As one raises the toroidal field, the resonant layer at which $\omega_{\text{laser}} = 3\omega_C$ for a given line moves from inside of the toroidal axis ($r < 0$) to the outside ($r > 0$). At still higher fields, the second harmonic layer enters the plasma from the inside and moves toward the center, with a third harmonic transmission near unity. The effect of translating the resonance layer across the plasma is demonstrated in fig. 4, for the toroidal field variation $7.5 < B_t$ (Tesla) < 10.5 . Also shown for comparison are Gaussian temperature profiles fit to Thomson scattering data at the lowest and highest fields present in the data, for the intermediate density of $2.0 \times 10^{14} \text{cm}^{-3}$.

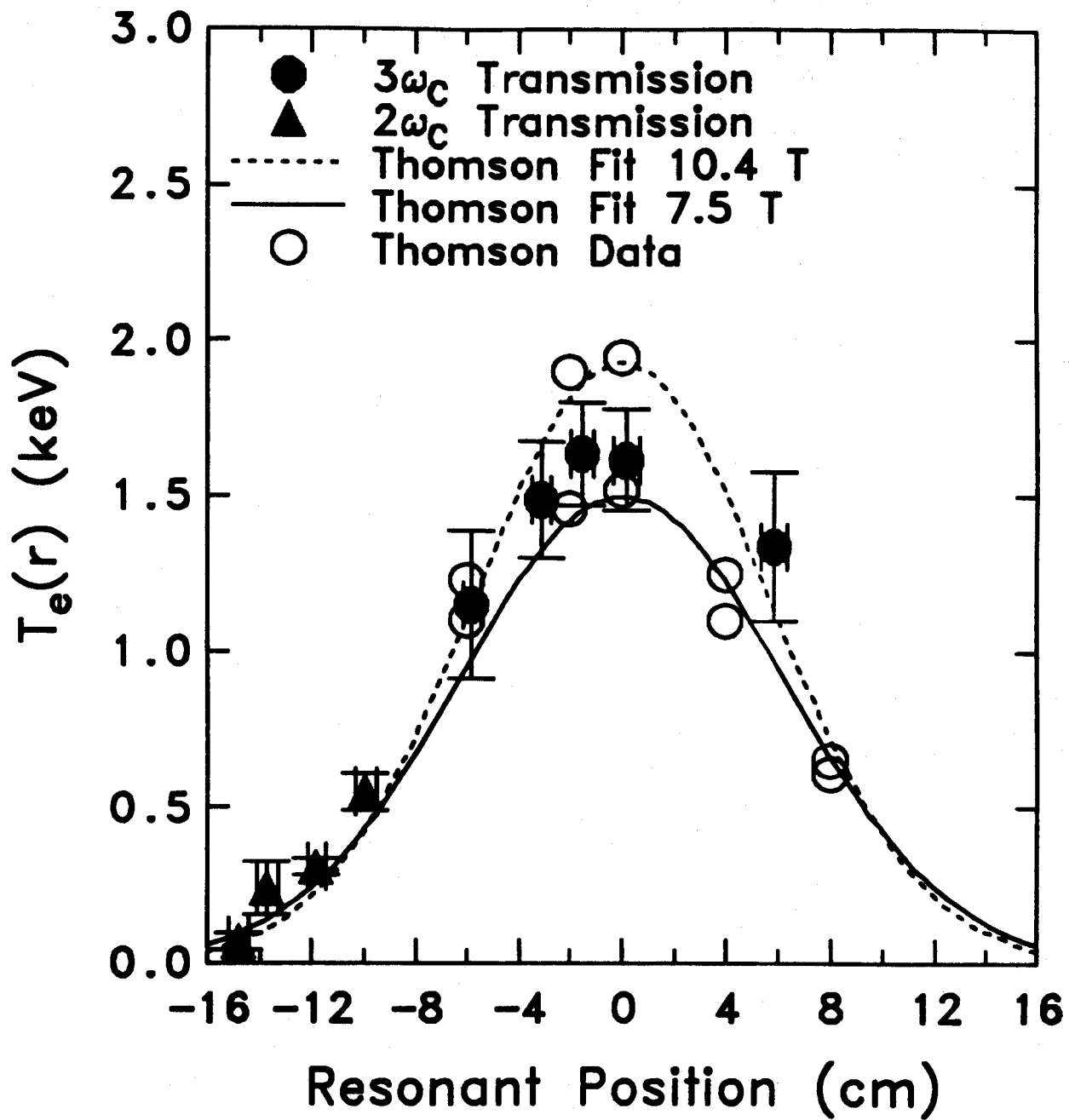
The entire 75 eV to 3.5 keV range of temperatures in figures 3 and 4 was measured by second or third harmonic cyclotron transmission with the same experimental arrangement and measurement technique along a single horizontal chord.



2. Parameter scaling of the third harmonic X mode optical depth.



3. Central temperature diagnostic performance of third harmonic X mode transmission measurements.

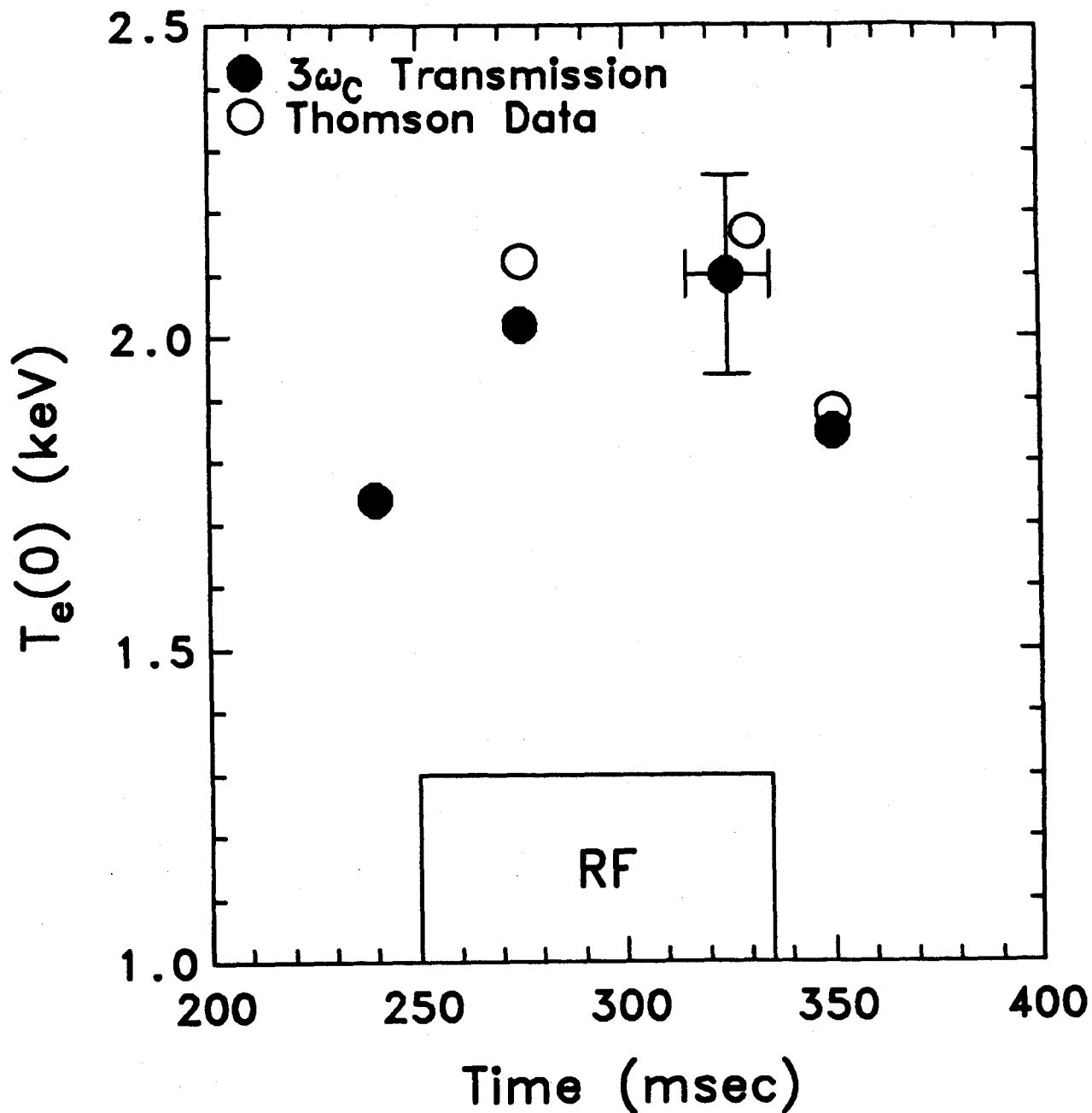


4. Electron temperature from second and third harmonic X mode transmission vs. Position. $B_t = 7.5 - 10.4$ T, $\bar{n}_e = 1.6 - 2.4 \times 10^{14}$ cm $^{-3}$, $I_p = 450$ kA, $q_t = 3.4 - 4.7$, $\lambda = 432.6$ μ m.

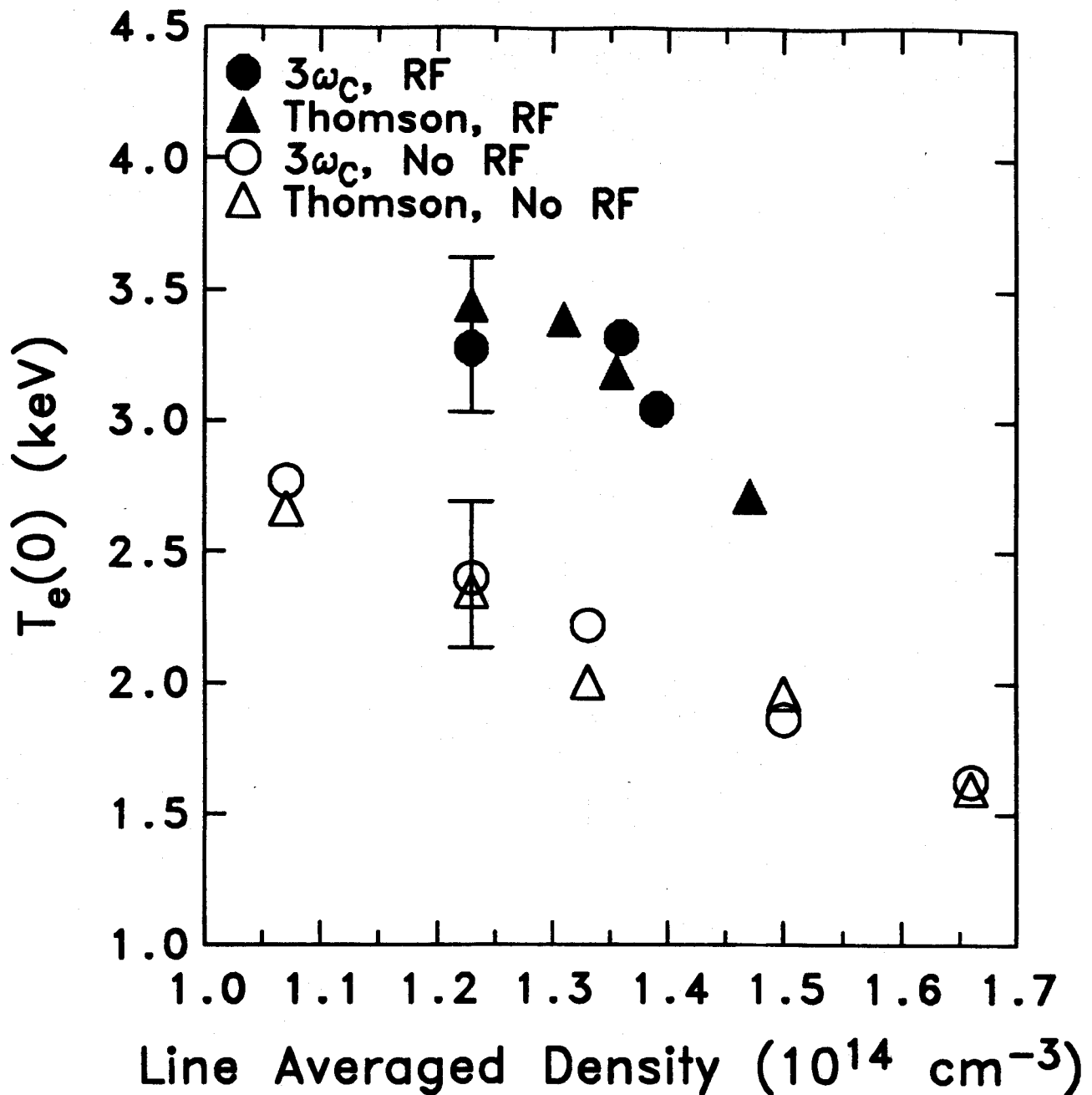
Unlike cyclotron emission based methods which are strongly affected by suprathermal emission during RF injection, cyclotron harmonic transmission measurements are ideal for diagnosing RF heated plasmas. The transmission technique produces continuous data, and features essentially local absorption. These attributes have allowed the observation of Sawtooth and $m=1$ MHD activities on the raw third harmonic transmission signal. These behaved in a manner well correlated with other diagnostics of MHD activity [6].

Temperature diagnostic operation during Lower Hybrid RF heating at 4.6 GHz [4] is demonstrated in fig. 5, for densities in the range $1.6 < \bar{n}_e(10^{14}\text{cm}^{-3}) < 2.0$, RF powers in the range $500 < P_{RF}(\text{kW}) < 700$, and Molybdenum limiters. Temperatures obtained from the $3\omega_C$ transmission data are shown as a function of time, along with Thomson scattering results. During the RF pulse the transmission data indicates an increase of 360 eV over the pre-RF value. The effect of Lower Hybrid RF Heating with Silicon Carbide limiters in plasmas with $1.2 < \bar{n}_e(10^{14}\text{cm}^{-3}) < 1.5$, $B_t = 9$ T, and 800 kW RF power is shown in fig. 6. Temperatures obtained from $3\omega_C$ transmission and Thomson scattering are plotted versus electron density, for plasmas with RF injection and without. Under these conditions, a maximum temperature rise of over 1 keV is observed.

If the RF power spectrum is not symmetric in k_{\parallel} , net momentum is coupled to the electron distribution, and a steady current can be driven solely by the action of the Lower Hybrid waves [5]. Because of difficulties brought by low absorption in the tenuous Current Drive plasma, transmissions during Current Drive are obtained by averaging over the steady portion of the RF pulse, and over nominally identical shots. For Current Drive flattop shots with $\pi/2$ phasing, $B_t = 8$ T, $3 < \bar{n}_e(10^{13}\text{cm}^{-3}) < 8$, and $125 \leq I_p(\text{kA}) \leq 145$, experimental transmissions were observed to be within 3% of the expected values, consistent with the accuracy of the measurements. In addition, no systematic difference was found between the absorption during RF injected shots and comparable Ohmic Simulations, in which the Ohmic current and density are programmed to duplicate Current Drive conditions in the absence of RF. Such shots provide a direct comparison of discharge



5. Electron temperature from third harmonic X mode transmission during RF Heating with Mo limiters vs. Time. D_2 fill gas, $B_t = 8$ T, $\bar{n}_e = 1.6 - 2.0 \times 10^{14} \text{ cm}^{-3}$, $I_p = 400 - 500$ kA, $\lambda = 432.6 \text{ } \mu\text{m}$, $P_{RF} = 500 - 700$ kW.

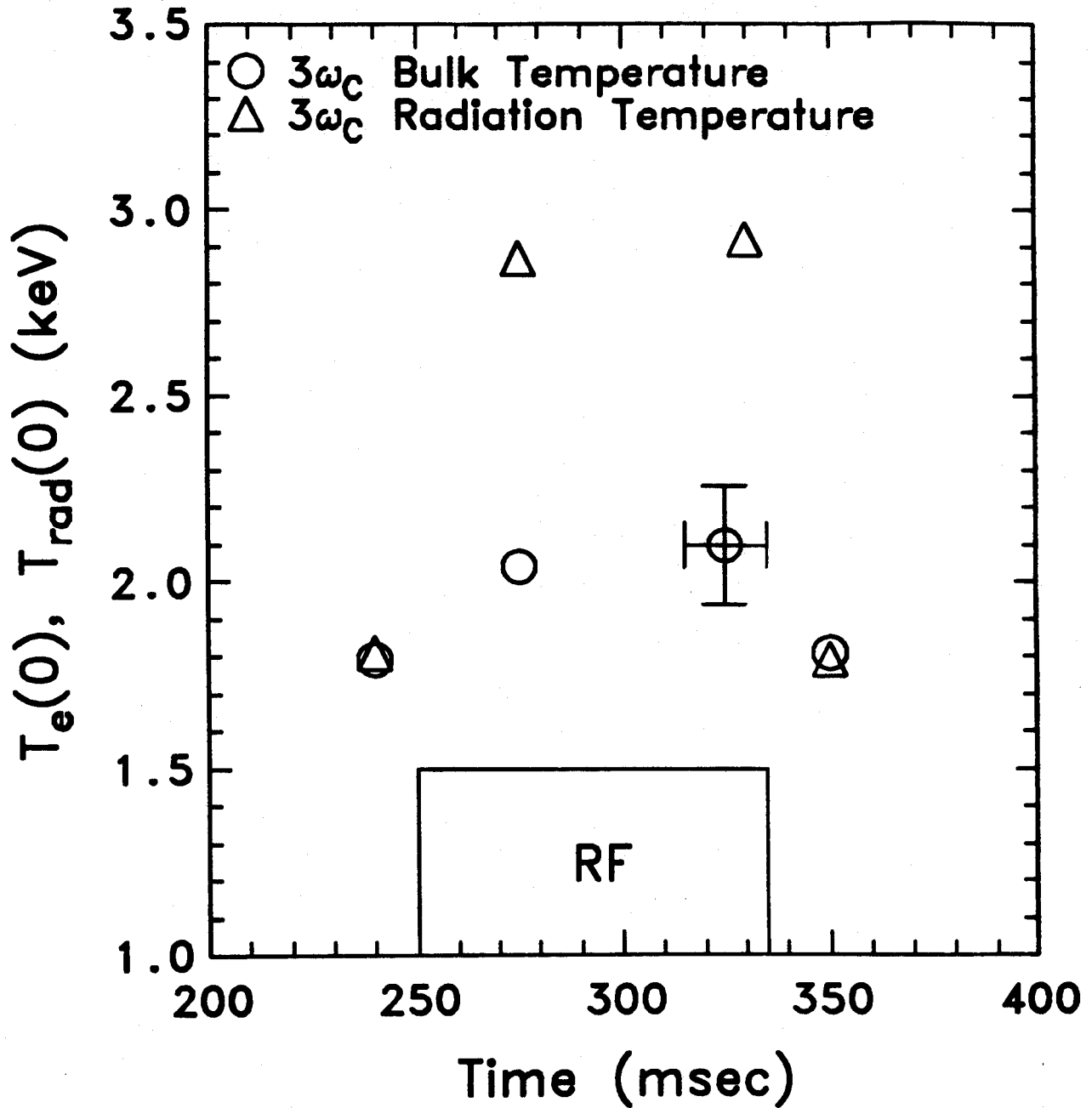


6. Electron temperature from third harmonic X mode transmission during RF Heating with SiC limiters vs. Density. D_2 fill gas, $B_t = 9$ T, $I_p = 410$ kA, $\lambda = 432.6 \mu\text{m}$, $P_{RF} = 800$ kW.

characteristics with and without the RF waves. Absorption of the suprathermal component is thus less than the accuracy of the determination, if present at all. This is in agreement with theoretical computations which indicate absorptions of less than 1% for a wide variety of Maxwellian class distribution functions with a tenuous, energetic electron population [6].

Application of the Equation of Transfer [7] during the beam modulation cycle leads to a system of equations which relate the $3\omega_C$ transmission and source function to the measured emission and transmission signals and the plasma chamber wall reflectivity [6]. Concurrent emission and transmission data thus allow a direct determination of the source function or radiation temperature, T_{rad} , to within a constant calibration factor. The behavior of the radiation temperature is most dramatic during RF heating, as shown in fig. 7, for the RF Heating run of fig. 5. T_{rad} was calibrated at 240 msec with T_e derived from the $3\omega_C$ transmission before the RF pulse, when T_{rad} and T_e are nearly equal. During the RF pulse, a large increase in the radiation temperature is observed relative to the thermal temperature, due to enhanced emission from suprathermal electrons produced by the RF waves. After the RF pulse terminates, the plasma quickly re-thermalizes, and T_{rad} once again equals T_e .

Transmission through the plasma may be accompanied by an attenuation which is independent of the occurrence of an $n\omega_C$ layer along the ray path. In ALCA-TOR C, two types of non-resonant attenuation have been observed. The first is associated with the appearance of a Marfe, as discussed previously. The second type of non-resonant attenuation observed is constant during most of the shot at a level of 5 to 30%, and is distinct from Marfe related effects. The attenuation scales strongly with the maximum electron density reached during the shot, although it exhibits little dependence on the instantaneous central density or temperature, toroidal field, or RF injection conditions. Although the existence of a source of non-resonant attenuation posed an additional complication in the analysis of transmission data, the apparent weak dependence on the time evolution of central plasma parameters and other conditions allowed a non-resonant correction to be obtained



7. $3\omega_C$ radiation temperature during Lower Hybrid RF Heating vs. Time. Mo limiters, D_2 fill gas, $B_t = 8$ T, $\bar{n}_e = 1.8 \times 10^{14} \text{ cm}^{-3}$, $I_p = 440$ kA, $\lambda = 432.6 \mu\text{m}$, $P_{RF} = 610$ kW.

consistently for a given experiment environment, using a number of methods, and applied to the transmission data. Methods of obtaining a non-resonant correction factor for use in the temperature analysis included monitoring the transmission of a non-resonant laser line, lowering the toroidal magnetic field by 10% to move the resonance to a plasma region where near unity transmission is expected, and comparisons with other temperature diagnostic data.

Due to physical constraints which arise from the experiment geometry, the highly collimated probe beam was constrained to lie within 1 cm of the plasma center. In this configuration a significant non-resonant attenuation cannot arise due to plasma refraction [6]. To estimate the effect of possible turbulent edge filamentation on the cyclotron harmonic transmission, the effect was treated as a random walk refraction by filamentary density clumps [8] which appear in the turbulence. Using this model, attenuations of up to 50% were obtained for various values of the edge density, fluctuation level, and turbulent layer thickness [6]. It is thought that edge turbulence may have caused the Gaussian probe beam to diverge slightly, and that this divergence caused a decrease in the observed transmission due to the small collection aperture accommodated by the constricted geometry of ALCATOR C.

4. Conclusions

Extraordinary mode transmission measurements at the semi-opaque second and third cyclotron harmonics are of unique diagnostic value in high temperature, high density Tokamak plasma research. With standard electron density and magnetic field data which are generally available in Tokamaks, the electron temperature can be obtained with an accuracy, spatial resolution and range which is comparable to the performance of existing temperature diagnostic techniques. Furthermore, with emission data which is concurrently available in the ECA measurements, the scaling of the radiation temperature may be directly obtained.

The fundamental physical principles governing the cyclotron absorption process endow the ECA diagnostic scheme with numerous unique attributes which make it

complementary to other temperature diagnostic methods. These include capabilities which remain unaffected by a wide variety of generic Maxwellian class suprathermal electron distributions, and performance which improves with increasing temperature. These characteristics make the ECA technique suitable for diagnosing RF heated plasmas, and also qualify the ECA technique for use as a temperature diagnostic in future devices. The ECA technique can also be applied to measure the local electron density, if temperature data is available, or local density-temperature products if neither density nor temperature are available. Where the second harmonic is semi-opaque, direct measurements of local plasma pressure may thus be obtained. This technique has been used in measuring the local pressure near the plasma edge, where neither accurate density nor accurate temperature data are available.

A number of limitations on the use of the ECA technique stem from the same physical and practical considerations which give the technique its usefulness. Implementation of the ECA temperature measurement technique requires a far infrared source, and is dependent on the existence and accuracy of electron density and magnetic field data. The accuracy of the temperature determination degrades rapidly for conditions of low density or temperature, due to the low absorption. Plasma variations on the modulation timescale or faster are averaged out in the analysis, and the analysis routine itself is sensitive to transient noise. These features make the temperature diagnostic technique difficult to apply to very tenuous or noisy plasmas, or to RF Current Drive plasmas, which are generally both noisy and tenuous. Furthermore, the appearance of Marfes at high densities provides an additional complication, and may preclude using the ECA technique during solid pellet fueling, which frequently precipitates Marfe activity. Marfe conditions, however, are spatially localized and readily identified using standard Tokamak diagnostics, and are thus in principle readily avoided.

A remaining drawback lies in the possible existence of a non-resonant attenuation which may complicate the implementation of the ECA diagnostic technique. In temperature diagnostic applications, the non-resonant attenuation characteristics

should be investigated in the regime, device, and geometry of interest. Increasing the collection aperture relative to the probe beam diameter may help eliminate any effects caused by a slight broadening of the beam. In cases where a significant NRA is found, capabilities should be developed early on to provide adequate correction data. This could be accomplished [6] using either the methods described above, or with simultaneous multiple harmonic operation of a Gyrotron [9] or Free Electron Laser [10] source. It is also important to have adequate Marfe and edge plasma diagnostics located at the site of the optical path to clearly monitor these phenomena, which may have a dramatic effect on the submillimeter wave transmission.

ACKNOWLEDGEMENTS

The authors wish to thank Dr. Stephen Tamor of Science Applications, Inc. for providing access to the computer codes used to study the absorption of cyclotron harmonic radiation by suprathreshold electron components. The assistance and participation of the ALCATOR group is also gratefully acknowledged. This work was supported by the U.S. Department of Energy, Contract No. DE-AC02-78ET51013.

REFERENCES

1. Bornatici, M., Cano, R., De Barbieri, O., Engelmann, F., *Nucl. Fusion* **23**,9 (1983) 1153, and references therein.
2. Engelmann, F., Curatolo, M., *Nucl. Fusion* **13** (1973) 497.
3. Lipschultz, B., LaBombard, B., Marmar, E. S., Pickrell, M. M., Terry, J. L., Watterson, R., Wolfe, S. M., *Nucl. Fusion* **24** (1984) 977.
4. Porkolab, M., Lloyd, B., Takase, Y., Bonoli, P. T., Fiore, C., Gandy, R., Granetz, R., Griffin, D., Gwinn, D., Lipschultz, B., Marmar, E., McCool, S., Pachtman, A., Pappas, D., Parker, R., Pribyl, P., Rice, J., Terry, J., Texter, S., Watterson, R., Wolfe, S., *Phys. Rev. Letters* **53**,13 (1984) 1229.
5. Porkolab, M., Schuss, J. J., Lloyd, B., Takase, Y., Texter, S., Bonoli, P. T., Fiore, C., Gandy, R., Gwinn, D., Lipschultz, B., Marmar, E., Pappas, D., Parker, R., Pribyl, P. *Phys. Rev. Letters* **53**,5 (1984) 450.
6. Pachtman, A., "Extraordinary Mode Absorption at the Electron Cyclotron Harmonic Frequencies as a Tokamak Plasma Diagnostic", MIT Plasma Fusion Center Report PFC/RR-86-22, Cambridge, Massachusetts, September, 1986.
7. Bekefi, G., "Radiation Processes in Plasmas" John Wiley and Sons, 1966, page 41.
8. Zweben, S. J., McChesney, J., Gould, R. W., *Nucl. Fusion* **23**,6 (1983) 825.
9. Byerly, J. L., Danly, B. G., Kreischer, K. E., Temkin, R. J., Mulligan, W. J., Woskoboinikow, P., *Int. J. Electronics* **57**,6 (1984) 1033. Also see Danly, B. G., Mulligan, W. J., Temkin, R. J., Sollner, T. C. L. G., *Applied Phys. Letters* **46**,8 (1985) 728.
10. Davidson, R. C., *Phys. Fluids* **29**,1 (1986) 267.

FIGURE CAPTIONS

1. Experiment configuration and components. Shown are the injection geometry, Tokamak cross section, waveguide assemblies, and filtering and detection assemblies.
2. Parameter scaling of the third harmonic X mode optical depth.
3. Central temperature diagnostic performance of third harmonic X mode transmission measurements.
4. Electron temperature from second and third harmonic X mode transmission vs. Position. $B_t = 7.5 - 10.4$ T, $\bar{n}_e = 1.6 - 2.4 \times 10^{14}$ cm⁻³, $I_p = 450$ kA, $q_t = 3.4 - 4.7$, $\lambda = 432.6$ μ m.
5. Electron temperature from third harmonic X mode transmission during RF Heating with Mo limiters vs. Time. D₂ fill gas, $B_t = 8$ T, $\bar{n}_e = 1.6 - 2.0 \times 10^{14}$ cm⁻³, $I_p = 400 - 500$ kA, $\lambda = 432.6$ μ m, $P_{RF} = 500 - 700$ kW.
6. Electron temperature from third harmonic X mode transmission during RF Heating with SiC limiters vs. Density. D₂ fill gas, $B_t = 9$ T, $I_p = 410$ kA, $\lambda = 432.6$ μ m, $P_{RF} = 800$ kW.
7. $3\omega_C$ radiation temperature during Lower Hybrid RF Heating vs. Time. Mo limiters, D₂ fill gas, $B_t = 8$ T, $\bar{n}_e = 1.8 \times 10^{14}$ cm⁻³, $I_p = 440$ kA, $\lambda = 432.6$ μ m, $P_{RF} = 610$ kW.